arXiv:1410.0726v3 [stat.CO] 12 Jun 2016

co-BPM: a Bayesian Model for Estimating Divergence and Distance of Distributions

Kun Yang[1], Hao Su[2], and Wing Hung Wong[3]

[1]Institute of Computational and Mathematical Engineering, Stanford University
[2]Department of Computer Science, Stanford University
[3]Department of Statistics, Stanford University
[3]Department of Health Research and Policy, Stanford University

Abstract

Regarding each instance as an independent draw from continuous probability distributions, divergence estimation is applied to important problems such as low-dimensional embedding, manifold learning, clustering, classification, and anomaly detection. We proposed a Bayesian model to characterize the discrepancy of two samples, e.g., to estimate the divergence or distance of their underlying distributions. The core idea of this framework is to learn a partition of the sample space that best captures the landscapes of their distributions. In order to avoid the pitfalls of plug-in methods that estimate each sample density independently with respect to the Lebesgue measure, we make direct inference on the two distributions simultaneously from a joint prior, i.e., the coupled binary partition prior. Our prior leverages the class of piecewise constant functions built upon binary partitions of the domain. Our model provides a unified way to estimate various types of discrepancies between samples and enjoys convincing accuracy. We demonstrate its effectiveness through simulations and comparisons with the *state-of-the-art*.

Key Words: coupled binary partition, divergence, MCMC, variance reduction

1 Introduction

The question of how to understand the discrepancy between two samples is of fundamental importance in various disciplines such as statistics, information theory and machine learning.

In statistics, hypothesis testing procedures such as Kolmogorov-Simirnov test and Cramer-von Mises test are based on some discrepancy measurement of the empirical distributions, and a common goal in Bayesian experimental design (Chaloner and Verdinelli, 1995) is to maximize the expected Kullback-Leibler (KL) divergence between the prior and the posterior. In information theory, divergence plays an important role since other information theoretic quantities such as mutual information and Shannon Entropy are derived from it. In machine learning, probability distance measures such as Total Variation, Hellinger Distance and KL divergence are often applied as a loss function in manifold learning (Donoho and Grimes, 2003), classification and anomaly detection, etc. For instance, it is applied to image registration and multimedia classification problems as a similarity measure (Ho and Vasconcelos, 2004).

Estimating discrepancies of two probability distributions, especially KL divergence, based on a set of observations from each distribution has a long history and rich literature. For ease of elaboration, we formulate the problem in mathematical terms: given the sample space Ω, two sets of i.i.d observations $\mathcal{X} = \{x_i\}_{i=1}^{n_1}$ and $\mathcal{Y} = \{y_i\}_{i=1}^{n_2}$ are generated from probability measures P_1 and P_2 with densities $p_1(x)$ and $p_2(y)$ respectively. Various measures of discrepancy of p_1 and p_2 have the following general form

$$D_\phi(p_1, p_2) = \int p_1(x)\phi\Big(\frac{p_2(x)}{p_1(x)}\Big)dx$$

where ϕ is a convex function. D_ϕ is the class of Ali-Silvey distances (Ali and Silvey, 1966), also known as $f-$divergences. Many common divergences, such as KL divergence ($\phi(x) = -\log(x)$), $\alpha-$divergence (e.g., $\phi(x) = 4/(1-\alpha^2)\cdot(1-x^{(\alpha+2)/2})$ when $\alpha \neq \pm 1$), Hellinger distance ($\sqrt{D_\phi}$ and $\phi(x) = 1-\sqrt{x}$), and total variation distance ($\phi(x) = |x-1|$), are special cases of $f-$divergence, coinciding with a particular choice of f.

We are interested in estimating D_ϕ from two samples $\mathcal{X}$ and $\mathcal{Y}$, without any assumptions of the forms of p_1 and p_2. A conceptually simple approach is to proceed in two-steps: estimate the densities $\hat{p}_1$ and $\hat{p}_2$ according to the $\mathcal{X}$ and $\mathcal{Y}$ independently then calculate $D_\phi(\hat{p}_1, \hat{p}_2)$. However, this method is unattractive for the following reasons: i) multivariate density estimation itself is a challenging problem and often more difficult than comparing distributions, so poorly estimated densities can cause subsequent discrepancy estimation to suffer from high variance and bias (Ma and Wong, 2011); ii) if the first stage is carried out independently, there is no easy way to compute their discrepancy $D_\phi(\hat{p}_1, \hat{p}_2)$ analytically; some numeric or approximation routines have to be employed, which in turn introduce more error terms (Sugiyama et al., 2012). Hence, throughout this paper, we focus on the class of single-shot methods, i.e., comparing samples directly and simultaneously.

We review several methods in the context of information theory and machine learning. Interested readers may refer to (Sricharan et al., 2010; Wang et al., 2009; Leonenko et al., 2008; Póczos and Schneider, 2011; Ma and Wong, 2011; Póczos et al., 2012) for other recent developments. (Wang et al., 2005) proposes a domain-splitting method that constructs an

adaptive partition of the sample space with respect to $\mathcal{Y}$, then Radon-Nikodym derivative $p_1(x)/p_2(x)$ can be estimated with empirical probability mass (with the correction term on the boundary) in each sub-region. In 1-dimension, strong consistency is established and several algorithmic refinements are suggested. In multi-dimensions, a partitioning scheme is also mentioned based on the heuristics in 1-dimensional case, however, there are not enough numeric simulations to justify the heuristics. (Nguyen et al., 2010) derives a variational characterization of the $f-$divergence in terms of a Bayes decision problem, which is exploited to develop an $M-$estimator. The theoretical results of consistency and convergence rates are provided. It is also shown that the estimation procedure can be cast into a finite-dimensional convex program and solved efficiently when the function class is defined by reproducing kernel Hilbert spaces. (Sugiyama et al., 2012) introduces the least-squares density-difference (LSDD) estimator is developed in the framework of kernel regularized least-squares estimation. The finite sample error bound shows that LSDD achieves the optimal convergence rate. They also demonstrate several pattern recognition applications.

Despite of the success of these methods, they are insufficient in many scenarios. For example, since $\mathcal{X}$ and $\mathcal{Y}$ are two sets of random observations, one may be interested in the confidence (credible) intervals of estimated discrepancies (Sricharan et al., 2010), but deriving such quantities are non-trivial for these methods. Secondly, these methods and theories are all set up for a specific type of discrepancy and are usually not directly applicable to others. Thirdly, to the best of our knowledge, few experiments are conducted in dimensions larger than 3 in previous work (Sricharan et al., 2010; Nguyen et al., 2010; Pérez-Cruz, 2008), even though most of the methods claim that there are no technical difficulties as one increases the number of dimensions. Finally, there is little work on tackling discrepancy estimation under the Bayesian perspective.

In this paper, we introduce a single-shot Bayesian model, which we name as **co**upled **B**inary **P**artition **M**odel (co-BPM). Our model design is inspired by two key ideas. First, we use an adaptive partitioning scheme, which has been demonstrated to be more scalable (see Table 1) than traditional domain splitting methods such as histogram (Wang et al., 2005) or regular paving (Sainudiin et al., 2013). Second, instead of partitioning based upon $\mathcal{Y}$ alone as in (Wang et al., 2005), we force the domain Ω to be *coupled* so that it is partitioned with respect to $\mathcal{X}$ and $\mathcal{Y}$ simultaneously. Therefore, our model is capable of capturing the landscape of both $\mathcal{X}$ and $\mathcal{Y}$, thus is more effective in estimating their discrepancies.

We highlight our contributions as follows:

1. To our knowledge, co-BPM is the first *single-shot domain-partition* based Bayesian model for discrepancy estimation, that is scalable in both dimension and sample size.

2. The specifically tailored MCMC sampling algorithm exploits the sequential buildup of binary partition for rapid mixing.

3. The method is tested in 5 and 10 dimensional settings that are rare in previous work.

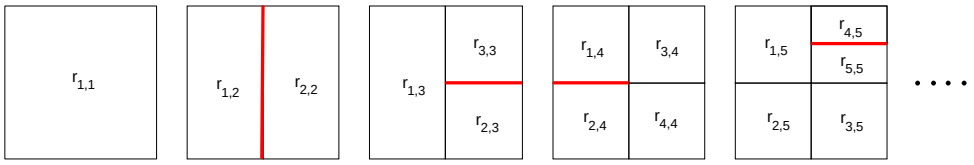

Figure 1: A **binary partition sequence** demonstrates its sequential structure. Each red line indicates the decision to halve the sub-rectangle alone it.

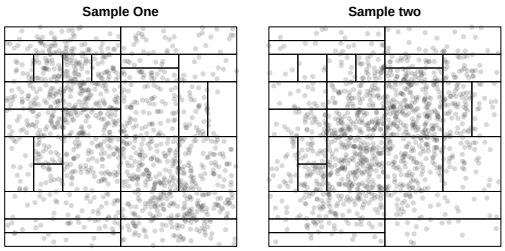

Figure 2: An illustration of **coupled binary partition** of two samples through the coupled binary partition model. Two samples are drawn from two different distributions and their sampling spaces are partitioned in tandem.

Experiments show that we achieve better convergence and higher accuracy than other methods.

4. We propose two *variance reduction* approaches that are effective for discrepancies involving divisions (e.g., in $\alpha-$divergence).

We validate our model by intensive simulations: 1) two sanity tests are used to demonstrate that our model is sensitive to the differences among samples; 2) a 4-dim example is used to demonstrate the effectiveness of variance reduction; 3) examples in 5-dim and 10-dim are carried out and are compared to the methods in (Nguyen et al., 2010) and (Pérez-Cruz, 2008)

The rest of the paper is organized as follows: Section 2 introduces some notations used throughout our discussion and preliminaries that motivate our model; Section 3 introduces the Coupled Binary Partition Model and the specially tailored MCMC algorithm to sample posterior effectively; extensive simulations and comparisons are presented in Section 4; we draw the conclusions in Section 5.

2 Notation and Preliminaries

Throughout the paper, we assume $\Omega = [0,1]^d$ and consider the domain-splitting approach to estimate the discrepancies through coordinate-wise binary partition. A binary partition has hierarchical structure that is constructed sequentially: starting with $\mathcal{B}_1 = \{r_{1,1} = \Omega\}$ at depth 1, action a_1 is taken to split Ω into $\mathcal{B}_2 = \{r_{1,2}, r_{2,2}\}$ along the middle of one of its coordinates; then at depth 2, action a_2 is taken to split one of sub-rectangles in B_2 into $\mathcal{B}_3 = \{r_{1,3}, r_{2,3}, r_{3,3}\}$ evenly. The process keeps on till the specified depth is reached. Given the maximum depth l, the decision sequence is denoted as $A_l = (a_1, ..., a_{l-1})$. A_l uniquely determines a split of Ω, which is denoted as $\{r_{1,l}, ..., r_{l,l}\}$. It is necessary to point out that multiple decision sequences may result in the same partition. An important property of binary partition motivates our coupling scheme in the following section. Figure 1 gives an illustration of the sequence in $[0,1]^2$; Figure 2 demonstrates the coupled binary partition, where the domains of two different samples are partitioned in tandem.

Property 1. *For any pair of decision sequences A_{l_1} and A_{l_2} and their partitions $\{r_{i,l_1}\}_{i=1}^{l_1}$ and $\{r_{i,l_2}\}_{i=1}^{l_2}$, there exists a sequence A_l and its partition $\{r_{i,l}\}_{i=1}^{l}$ such that r_{i,l_k} is the union of a subset of $\{r_{i,l}\}_{i=1}^{l}$ for $k = 1, 2$ and $i = 1, ..., l_k$, namely, A_l defines a more refined partition than A_{l_1} or A_{l_2}.*

The next theorem shows that a partition of Ω gives a lower bound of the discrepancies.

Theorem 1. *Given a partition $\{r_{1,l}, ..., r_{l,l}\}$ of Ω at depth l, let*

$$\tilde{p}_i(x) = \sum_{k=1}^{l} \frac{P_i(r_{k,l})}{|r_{k,l}|} \mathbf{1}\{x \in r_{k,l}\}$$

where $i = 1, 2$ and $|\cdot|$ denotes the volume or size, then

$$D_\phi(p_1, p_2) \geq D_\phi(\tilde{p}_1, \tilde{p}_2) \tag{1}$$

namely, a partition gives a way to estimate D_ϕ.

Remark 2.1. Another lower bound (Nguyen et al., 2010) of D_ϕ is $\sup_{f \in \mathcal{F}} \int [f dP_2 - \phi^*(f) dP_1]$, where $\mathcal{F}$ is a class of functions and ϕ^* is the conjugate dual function of ϕ. Theorem 1 shifts the difficulty of estimation from finding a good $\mathcal{F}$ to a good partition.

Remark 2.2. Under the condition that the integral $D_\phi(p_1, p_2)$ is Riemann integrable. It is trivial to show that $D_\phi(p_1, p_2) = \sup D_\phi(\tilde{p}_1, \tilde{p}_2)$, where the supremum is taken over all possible partitions on all depths.

The proof is straightforward by applying the Jensen's inequality.

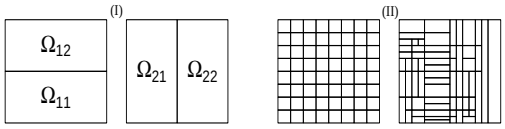

	$D_{q=1}$	$D_{q=2}$	$D_{\alpha=1}$	$D_{\alpha=2}$
Hist	0.5269	0.4935	0.7964	1.0291
BP	**0.5431**	**0.4990**	**0.8267**	**1.0527**
Truth	0.5518	0.5204	0.8604	1.0769

Table 1: **A simple illustration demonstrates the importance of a good partition.** (I) $\mathcal{B}_1 = \{\Omega_{11}, \Omega_{12}\}$ and $\mathcal{B}_2 = \{\Omega_{21}, \Omega_{22}\}$ are two partitions of unit cube. Consider $p_1(x) = \frac{3}{2}\mathbf{1}\{x \in \Omega_{11}\} + \frac{1}{2}\mathbf{1}\{x \in \Omega_{12}\}$ and $p_2(x) = \frac{1}{2}\mathbf{1}\{x \in \Omega_{11}\} + \frac{3}{2}\mathbf{1}\{x \in \Omega_{12}\}$. Under $\mathcal{B}_1$, the lower bounds equal $D_\phi(p_1, p_2)$, i.e., $D_\phi = \frac{3}{4}\phi(\frac{1}{3}) + \frac{1}{4}\phi(3)$. For instance, the Total Variation Distance is $\frac{1}{2}$, Hellinger Distance is $\frac{\sqrt{3}}{2} - \frac{1}{2}$ and $\alpha-$divergence is $\alpha = 2$ is $\frac{1}{\alpha-1}\log(\frac{3}{4}\cdot 3^{\alpha-1} + \frac{1}{4}\cdot\frac{1}{3}^{\alpha-1})$ respectively; however, under $\mathcal{B}_2$, the lower bounds are $\phi(1)$, where the Total Variation Distance, Hellinger Distance and $\alpha-$divergence with $\alpha = 2$ are all 0. (II) $p_1(x) = \beta_{3,5}(x_1)\beta_{3,5}(x_2)$ and $p_2(x) = \mathbf{1}\{x \in [0,1]^2\}$. On the left is histogram by dividing each dimension into 8 equal sub-intervals; on the right is an adaptive partition with 64 sub-rectangles. As summarized in the right table, **BP** (adaptive binary partition) is closer to **Truth** (the true values) than **Hist** (histogram).

Proof. We decompose the integral by $\{r_{1,l}, ..., r_{l,l}\}$ and apply Jensen's inequality,

$$\begin{aligned} D_\phi(p_1, p_2) &= \int_\Omega p_1(x)\phi\Big(\frac{p_2(x)}{p_1(x)}\Big)dx = \sum_{i=1}^{l}\int_{r_{i,l}} p_1(x)\phi\Big(\frac{p_2(x)}{p_1(x)}\Big)dx \\ &= \sum_{i=1}^{l} P_1(r_{i,l})E_{p_1(\cdot|r_{i,l})}[\phi\Big(\frac{p_2(x)}{p_1(x)}\Big)] \geq \sum_{i=1}^{l} P_1(r_{i,l})\phi\Big(E_{p_1(\cdot|r_{i,l})}\frac{p_2(x)}{p_1(x)}\Big) = \sum_{i=1}^{l} P_1(r_{i,l})\phi\Big(\frac{P_2(r_{i,l})}{P_1(r_{i,l})}\Big) \end{aligned} \tag{2}$$

□

Remark 2.2 indicates that the divergence can be defined over countable partitions. A simple illustration in Table 1 implies the importance of a good partition. In next section, we describe how Theorem 1 specializes to a partition based estimator for $f-$divergence.

A closer look into the proof of Theorem 1 gives us more insights. Let's take the derivation for D_ϕ as an example. Within each region, the gap between $D_\phi(p_1, p_2)$ and $D_\phi(\tilde{p}_1, \tilde{p}_2)$ comes from applying Jensen's inequality, therefore, it can be closed if $p_1(x)/p_2(x)$ in each region is approximately constant. Such observations indicate that partitioning the domain more finely would reduce the estimation bias. However, an overly fine partitioning will cause insufficient samples in each region and inadvertently increase the overall estimation variance. So there is a *trade-off between bias and variance*. Therefore, an appropriate partitioning respecting the tradeoff should reflect the landscape of $\mathcal{X}$ and $\mathcal{Y}$ simultaneously and avoid over-cutting. We will see how this intuition is implemented in our Bayesian model.

3 Coupled Binary Partition Model

In light of Theorem 1 and the importance of partitions, we model probability mass pairs $(P_1(r_{i,l}), P_2(r_{i,l}))_{i=1}^l$ directly for a given partition $\{r_{i,l}\}_{i=1}^l$. Since the lower bounds (1) need only $(P_1(r_{i,l}), P_2(r_{i,l}))_{i=1}^l$, once they are fixed, we restrict the density in each sub-rectangle to be constant to reduce the complexity of density class, i.e., the density class is piecewise constant functions supported on binary partitions.

Specifically, the prior is constructed as follows: 1) the decision sequence of depth $l \in \mathcal{N}^+$ has a prior density proportional to $\exp(-\sigma l)$ with some positive σ and that all sequences at the same depth are distributed uniformly—this part of the prior is to discourage over-cutting as discussed in the previous section; 2) given an decision sequence $A_l = (a_1, ..., a_{l-1})$ and the fact that $\sum_{i=1}^l P_k(r_{i,l}) = 1$ for $k = 1, 2$, the probability masses $(P_1(r_{i,l}))_{i=1}^l, (P_2(r_{i,l}))_{i=1}^l$, denoted as $\mathbf{m}_{1,l}, \mathbf{m}_{2,l}$ or $(m_{1i,l})_{i=1}^l, (m_{2i,l})_{i=1}^l$ have a Dirichlet prior $\mathrm{Dir}(\delta, ..., \delta)$ respectively with some positive δ and the priors are independent between samples $\mathcal{X}$ and $\mathcal{Y}$. Thus,

$$p(l, A_l, (\mathbf{m}_{1,l}, \mathbf{m}_{2,l})) \propto \exp(-\sigma l) \prod_{i=1}^l m_{1i,l}^{\delta-1} \prod_{i=1}^l m_{2i,l}^{\delta-1}$$

The densities are uniform conditioned on each sub-rectangle, i.e.,

$$\hat{p}_1(x) = \sum_{i=1}^l \frac{m_{1i,l}}{|r_{i,l}|} \mathbf{1}\{x \in r_{i,l}\}, \hat{p}_2(y) = \sum_{i=1}^l \frac{m_{2i,l}}{|r_{i,l}|} \mathbf{1}\{y \in r_{i,l}\}$$

As discussed in Section 1, a naive two step algorithm proceeds as follows: estimating two piecewise constant densities $\hat{p}_1$ and $\hat{p}_2$ supported on (different) binary partitions independently based on $\mathcal{X}$ and $\mathcal{Y}$; then computing $D_\phi(\hat{p}_1, \hat{p}_2)$, which requires to consider all the intersections of sub-rectangles between two partitions. The drawbacks of this type of approach are already discussed. However, according to Property 1, any two piecewise constant densities supported on different binary partitions can be rewritten such that they are defined on the same binary partition, thus we *couple* $\hat{p}_1, \hat{p}_2$ by partitioning their domain in tandem (i.e., forcing the same A_l) in the prior such that Theorem 1 is applicable. The difference of $\hat{p}_1, \hat{p}_2$ is captured by $\mathbf{m}_{1,l}, \mathbf{m}_{2,l}$.

The likelihood of $\mathcal{X}$ and $\mathcal{Y}$ is

$$p(\mathcal{X}, \mathcal{Y} | (l, A_l, (\mathbf{m}_{1,l}, \mathbf{m}_{2,l}))) = \prod_{i=1}^l \left(\frac{m_{1i,l}}{|r_{i,l}|}\right)^{n_{1i,l}} \prod_{i=1}^l \left(\frac{m_{2i,l}}{|r_{i,l}|}\right)^{n_{2i,l}}$$

where $(n_{ki,l})_{i=1}^l, k = 1, 2$ denotes the number of points in each region for samples $\mathcal{X}, \mathcal{Y}$. Under our assumption, the prior of $(\mathbf{m}_{1,l}, \mathbf{m}_{2,l})$ is distributed with joint Dirichlet distribution

$\mathrm{Dir}(\delta, ..., \delta) \times \mathrm{Dir}(\delta, ..., \delta)$. By denoting $\Theta = (l, A_l, (\mathbf{m}_{1,l}, \mathbf{m}_{2,l}))$, the posterior is

$$\begin{aligned} &p(\Theta = (l, A_l, (\mathbf{m}_{1,l}, \mathbf{m}_{2,l}))|\mathcal{X}, \mathcal{Y}) \propto p(\Theta)p(\mathcal{X}, \mathcal{Y}|\Theta) \\ &\propto \exp(-\sigma l) \prod_{i=1}^{l} \Big(\frac{1}{|r_{i,l}|}\Big)^{n_{1i,l}+n_{2i,l}} \prod_{i=1}^{l} (m_{1i,l})^{\delta+n_{1i,l}-1} \prod_{i=1}^{l} (m_{2i,l})^{\delta+n_{2i,l}-1} := \psi(\Theta|\mathcal{X}, \mathcal{Y}) \end{aligned} \tag{3}$$

Through sampling from the posterior, the discrepancies are estimated by $D_\phi(\hat{p}_1, \hat{p}_2)$.

3.1 Sampling

According to the decomposition in (3), the probability masses and the decision sequence are sampled hierarchically. The first step is to generate the depth l and decisions A_l. By marginalizing $\mathbf{m}_{1,l}$ and $\mathbf{m}_{2,l}$ in (3), (A_l, l) is distributed as

$$p(A_l, l|\mathcal{X}, \mathcal{Y}) \propto \exp(-\sigma l)\beta((\delta + n_{1i,l})_{i=1}^{l})\beta((\delta + n_{2i,l})_{i=1}^{l}) \prod_{i=1}^{l} \Big(\frac{1}{|r_{i,l}|}\Big)^{n_{1i,l}+n_{2i,l}} \tag{4}$$

where $\beta(\cdot)$ is the multinomial Beta function and defined as $\beta((z_i)_{i=1}^{k}) = \prod_{i=1}^{k} \Gamma(z_i)/\Gamma(\sum_{i=1}^{k} z_i)$ and $\Gamma(z)$ is the Gamma function. Furthermore, conditioned on l, A_l is distributed as

$$p(A_l|l, \mathcal{X}, \mathcal{Y}) \propto \beta((\delta + n_{1i,l})_{i=1}^{l})\beta((\delta + n_{2i,l})_{i=1}^{l}) \prod_{i=1}^{l} \Big(\frac{1}{|r_{i,l}|}\Big)^{n_{1i,l}+n_{2i,l}} \tag{5}$$

once A_l is generated, $\mathbf{m}_{1,l}$ and $\mathbf{m}_{2,l}$ are sampled through $\mathrm{Dir}((\delta + n_{1i,l})_{i=1}^{l})$ and $\mathrm{Dir}((\delta + n_{2i,l})_{i=1}^{l})$ respectively.

It is difficult to obtain the analytical distribution of (A_l, l) because of the intractability of normalizing constant or partition function, Markov Chain Monte Carlo is employed to sample the posterior (3). However, given the vast parameter space and the countless local modes, the naive Metropolis-Hastings (Hastings, 1970) suffers from slow mixing in our experience. In order to sample effectively, a proposal kernel should be chosen with the two properties: 1) it leverages the sequential structure of binary partition and the proposed partition is generated with respect to $\mathcal{X}$ and $\mathcal{Y}$ for rapid mixing; 2) the corresponding acceptance ratio depends on a smaller set of parameters; in other words, the transition probability is controlled by a subset of Θ, such that the size (dimensionality) of searching space is reduced. Define

$$g(\Theta' = (l', A_{l'}, (\mathbf{m}_{1,l'}, \mathbf{m}_{2,l'}))|\Theta = (l, A_l, (\mathbf{m}_{1,l}, \mathbf{m}_{2,l}))) = p(A_{l'}, l'|A_l, l)p((\mathbf{m}_{1,l'}, \mathbf{m}_{2,l'})|A_{l'}, l)$$

where $p(A_{l'}, l'|A_l, l) = p(l'|l)p(A_{l'}|A_l, l')$ defines the jump probability and l' is constrained to be $l - 1$ and $l + 1$. In order to exploit the sequential structure of binary partition such that

each a_l is drawn with the guidance of A_l, $p(A_{l+1}|A_l, l+1) = p(a_l|A_l, l+1)$ is defined as

$$\begin{aligned} p(a_l|A_l, l+1) &= \frac{p(A_{l+1}|l+1, \mathcal{X}, \mathcal{Y})}{p(A_l|l, \mathcal{X}, \mathcal{Y})} \\ &\propto \frac{\beta((\delta + n_{1i,l+1})_{i=1}^{l+1})\beta((\delta + n_{2i,l+1})_{i=1}^{l+1})}{\beta((\delta + n_{1i,l})_{i=1}^{l})\beta((\delta + n_{2i,l})_{i=1}^{l})} \frac{\prod_{i=1}^{l} |r_{i,l}|^{n_{1i,l}+n_{2i,l}}}{\prod_{i=1}^{l+1} |r_{i,l+1}|^{n_{1i,l+1}+n_{2i,l+1}}} \end{aligned} \tag{6}$$

and $p(A_{l-1}|A_l, l-1) = p(l-1|l)$ since $p(A_{l-1}|A_l, l-1) = 1$; $p((\mathbf{m}_{1,l'}, \mathbf{m}_{2,l'})|A_{l'}, l')$ is the joint Dirichlet distribution $\text{Dir}((\delta + n_{1i,l'})_{i=1}^{l'}) \times \text{Dir}((\delta + n_{2i,l'})_{i=1}^{l'})$. Thus, the acceptance ratio is

$$\begin{aligned} &Q(\Theta \to \Theta') = \min\{1, \frac{\psi(\Theta')g(\Theta|\Theta')}{\psi(\Theta)g(\Theta'|\Theta)}\} = \\ &\min\{1, \frac{\exp(\sigma l)\prod_{i=1}^{l} |r_{i,l}|^{n_{1i,l}+n_{2i,l}} p(A_l, l|A_{l'}, l')\beta((\delta + n_{1i,l'})_{i=1}^{l'})\beta((\delta + n_{2i,l'})_{i=1}^{l'})}{\exp(\sigma l')\prod_{i=1}^{l'} |r_{i,l'}|^{n_{1i,l'}+n_{2i,l'}} p(A_{l'}, l'|A_l, l)\beta((\delta + n_{1i,l})_{i=1}^{l})\beta((\delta + n_{2i,l})_{i=1}^{l})}\} \end{aligned} \tag{7}$$

where $\psi(\Theta|\mathcal{X}, \mathcal{Y})$ is defined in (3) and $\mathcal{X}, \mathcal{Y}$ are omitted to simplify notations. According to (7), $\mathbf{m}_{1,l}, \mathbf{m}_{1,l'}$ and $\mathbf{m}_{2,l}, \mathbf{m}_{2,l'}$ are canceled, $Q(\Theta \to \Theta')$ depends on (A_l, l) and $(A_{l'}, l')$ solely and avoids to searching the vast space of probability masses. Moreover, if $p(l'|l)$ is chosen to be symmetric, $Q(\Theta \to \Theta')$ can be further simplified.

In higher dimensions, sampling according to $p(A_{l'}|A_l, l')$ requires to count the number of points of $\mathcal{X}$, $\mathcal{Y}$ in each sub-rectangle of $A_{l'}$, which is expensive (with complexity $O((n_1 + n_2)d)$). If we are willing to run longer chains with cheaper cost per iteration, another heuristic choice for transition $p(A_{l'}, l'|A_l, l)$ is to increase or shrink A_l by one uniformly: $p(A_{l+1}, l+1|A_l, l) = p(l+1|l)/(l \cdot d)$ since there are $l \cdot d$ possible decisions (cutting locations), $p(A_{l-1}, l-1|A_l, l) = p(l-1|l)$ and $p(l+1|l) + p(l-1|l) = 1$ when $l > 1$; $p(A_{l+1}, l+1|A_l, l) = 1/(l \cdot d)$ when $l = 1$.

4 Numeric Simulations

4.1 Sanity Tests for co-BPM

We use two "sanity tests" to demonstrate that our model is sensitive to differences among samples, the densities used in experiments are two dimensional for ease of visualization. In the first group p_{11} and p_{12}, we force the mixture of p_{11} and p_{12} is uniformly distributed, i.e., $\frac{1}{2}(p_{11} + p_{12}) = \mathbf{1}\{x \in [0, 1]^2\}$; we generate 1,000 points each, thus the combined sample is equivalent to 2,000 points from uniform distribution; as shown in the first row of Figure 3, their difference is revealed by the partition well. The second group p_{21} and p_{22} are chosen such that they are both supported on the binary partition and p_{22} is defined on a finer partition than p_{21}; a good model should be able to produce the underlying partition, i.e.,

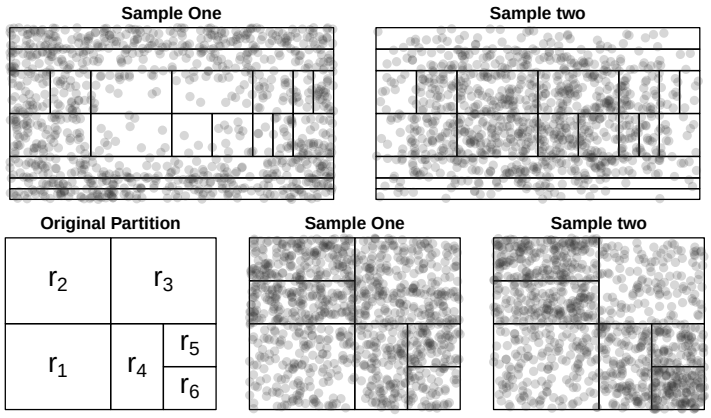

Figure 3: **Sanity Tests.** First row: 1,000 samples drawn from p_{11} and p_{21} and the learned partition; second row: 1,000 samples drawn from p_{21} and p_{22} and the learned partition.

find a density that is finer than both densities; the second row of Figure 3 shows this result.

$$p_{11}(x) = \frac{9}{5}\mathbf{1}\{x \in [0,1]^2\} - \frac{4}{5}\beta_{2,2}(x_1)\beta_{2,2}(x_2)$$

$$p_{12}(x) = \frac{1}{5}\mathbf{1}\{x \in [0,1]^2\} + \frac{4}{5}\beta_{2,2}(x_1)\beta_{2,2}(x_2)$$

$$p_{21}(x) = \frac{2}{3}\mathbf{1}\{x \in r_1\} + \frac{4}{3}\mathbf{1}\{x \in r_2\} + \mathbf{1}\{x \in r_3 \cup r_4 \cup r_5 \cup r_6\}$$

$$p_{22}(x) = \frac{2}{3}\mathbf{1}\{x \in r_1\} + \frac{4}{3}\mathbf{1}\{x \in r_2\} + \frac{1}{2}\mathbf{1}\{x \in r_3\} + \mathbf{1}\{x \in r_4\} + \frac{4}{3}\mathbf{1}\{x \in r_5\} + \frac{8}{3}\mathbf{1}\{x \in r_6\}$$

4.2 Simple Examples in 1 and 3 Dimensions

We demonstrate our methods by 2 simulations with dimension $d = 1, 3$ and size $n_1 = n_2 = 50, 250, 1250$. The parameters for co-BPM are $\delta = 1/2$ (which is the Jeffrey's non-informative prior), $\sigma = d + 1$, $p(l+1|l) = p(l-1|l) = 1/2$ for $l > 1$. The number of replicas for the box-plot is 3,000 and the burn-in number is 5,000. The discrepancies we consider are Total Variation, Hellinger Distance and KL divergence and $\alpha-$divergence with $\alpha = 2$. The true values of the discrepancies are obtained by Monte Carlo method with 10^8 samples.

1-dimensional examples. The densities are defined as below and the results are summarized in Figure 4.

$$p_1(x) = \beta_{6,5}(x), p_2(x) = \beta_{5,6}(x)$$

where $\beta_{a,b}(x)$ is the Beta distribution with shape parameters a, b.

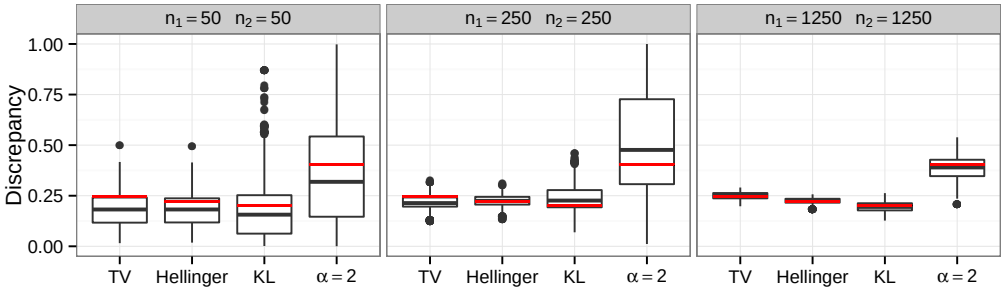

Figure 4: **1-dimensional simulation.** We draw 8,000 samples and generate box-plot after discarding the first 5,000 burn-in sample points. Theoretical discrepancies (red lines): 0.2461, 0.2207, 0.2000, 0.4056.

3-dimensional examples. The densities are defined as below and the results are summarized in Figure 5.

$$\begin{aligned} p_1(x,y,z) &= \frac{2}{5}\beta_{1,2}(x)\beta_{2,3}(y)\beta_{3,4}(z) + \frac{3}{5}\beta_{4,3}(x)\beta_{3,2}(y)\beta_{2,1}(z) \\ p_2(x,y,z) &= \frac{2}{5}\beta_{1,3}(x)\beta_{3,5}(y)\beta_{5,7}(z) + \frac{3}{5}\beta_{7,5}(x)\beta_{5,3}(y)\beta_{3,1}(z) \end{aligned} \tag{8}$$

It is observed from Figure 4 and 5 that co-BPM estimates the divergences reasonably well. Moreover, the estimation errors and variances are decreased when the sample size increases, so is the number of outliers in box-plots. According the histogram of depth l in Figure 5, another interesting observation is that the number of sub-rectangles increases in tandem with the sample size, which indicates that co-BPM refines the partitions to reveal more structure of the samples when more information becomes available, this multi-resolution property of binary partition is also discussed in Optional Pólya Tree (Wong and Ma, 2010).

The vanishing boundaries of beta distribution cause the large range and variance of KL and $\alpha-$divergence where division is involved, as demonstrated by the previous examples. Instead of using Jeffrey's noninformative prior, we choose a stronger prior with larger δ as a tradeoff between bias with variance. According to law of total variance, $\mathrm{Var}(m_{1i}) = E[\mathrm{Var}(m_{1i}|\mathcal{X})] + \mathrm{Var}[E(m_{1i}|\mathcal{X})]$. Since m_{1i} is generated from Dirichlet distribution, $\mathrm{Var}(m_{1i}|\mathcal{X}) = \frac{(n_{1i}+\delta)(n_1+\delta l-n_{1i}-\delta)}{(n_1+\delta l)^2(n_1+\delta l+1)} = O(\delta^{-1})$ and $\mathrm{Var}[E(m_{1i}|\mathcal{X})] = \mathrm{Var}(\frac{n_{1i}+\delta}{n_1+\delta l}) = \frac{\mathrm{Var}(n_{1i})}{(n_1+\delta l)^2}$; thus, asymptotically, its variance is reduced with a larger δ, as shown in Table 2.

4.3 Comparison with Other Methods

Most of other methods focus on KL divergence estimation. (Nguyen et al., 2010) derive a general lower bound for $f-$divergence via conjugate dual function; however, all of their theories and experiments are based on KL divergence estimation in 1, 2, 3 dimensions and

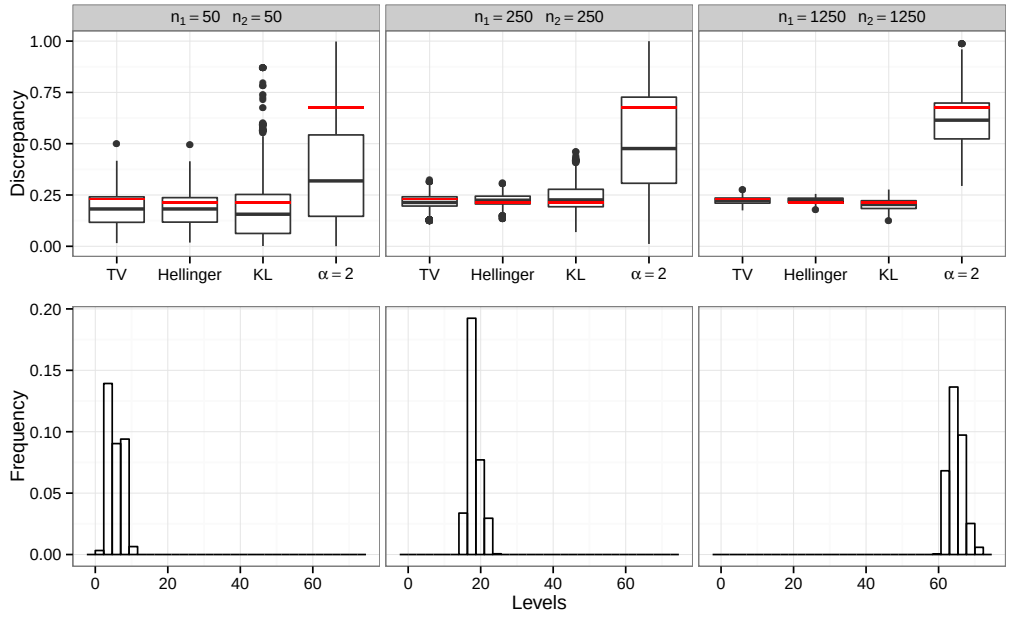

Figure 5: **3-dimensional simulation.** First row, box-plot with the same configuration as 1-dimensional case; theoretical discrepancies (red lines): 0.2301, 0.2129, 0.2133, 0.6769. Second row, we assess the behavior of depth l after discarding first 5,000 burn-in samples, the increase of number of sub-rectangles as sample size increases indicates that co-BPM refines the partitions when more information becomes available, which is analogous to the multi-resolution property discussed in (Wong and Ma, 2010).

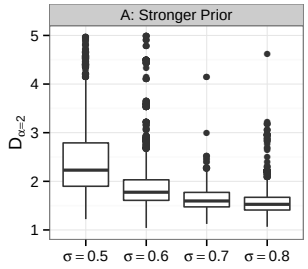

	Stronger Prior (δ)			
	0.5	0.6	0.7	0.8
Medians	2.3057	1.7771	1.5960	1.5267
Std	1.2690	0.6643	0.2223	0.2494

Table 2: **Illustration of bias and variance tradeoff.** $\mathcal{X} \sim \mathcal{N}(\mu_1 \mathbf{1}, \sigma_1^2 \mathbf{I})$, $\mathcal{Y} \sim \mathcal{N}(\mu_2 \mathbf{1}, \sigma_2^2 \mathbf{I})$ and are truncated in $[0,1]^4$, where $|\mathcal{X}| = |\mathcal{Y}| = 500$; $\mu_1 = 1/3, \mu_2 = 1/2$ and $\sigma_1 = 1/5, \sigma_2 = 1/5$; $\mathbf{1}$ is 4-dim unit vector and $\mathbf{I}$ is 4-dim identity matrix. As pseudo-count σ increases, the variance decreases and bias increases. True value: 2.2196. The table on the right lists the medians and standard errors.

their algorithms require that two samples have same size. In this section, we compare co-BPM to the methods in (Nguyen et al., 2010) and (Pérez-Cruz, 2008) in KL divergence estimation.

We briefly describe the methods in (Nguyen et al., 2010) and (Pérez-Cruz, 2008), interested readers may refer to the original papers for details. The core of (Nguyen et al., 2010)'s algorithm is a convex program that has the number of parameters equal to the sample size. As pointed out by the authors, the performance of the algorithm depends on a regularization parameter λ; here we choose λ according to their suggestions. There are two slightly different versions of KL estimator proposed, which are denoted by NWJ-M1 and NWJ-M2 in our experiments. On the other hand, the idea of (Pérez-Cruz, 2008)'s approach is relatively straightforward: the $k-$*nearest neighbor density estimate* is computed for each sample point in $\mathcal{X}$, i.e., $\hat{p}_1(x)$ and $\hat{p}_2(x)$ for $x \in \mathcal{X}$, then KL divergence is estimated by $\frac{1}{|\mathcal{X}|}\sum_{x\in\mathcal{X}} \log \frac{\hat{p}_1(x)}{\hat{p}_2(x)}$ (denoted by PC$-k$). Some more sophisticated algorithms are proposed based on $k-$nearest neighbor, e.g., (Póczos et al., 2012). The tuning parameter k is critical to guarantee their performance, we follow the choice of (Pérez-Cruz, 2008) by setting $k = 1$ and $k = 10$. One should also notice that the positivity of the estimates is not guaranteed.

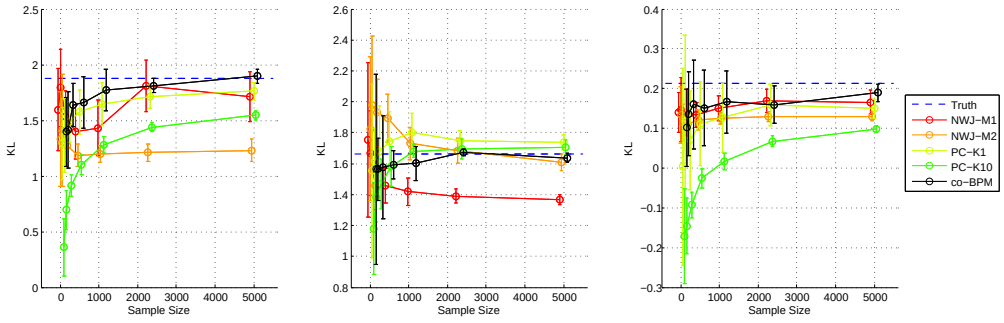

Figure 6: **Comparisons of NWJ, PC$-k$ and co-BPM.** All densities are truncated in $[0,1]^3$ and each line is slightly shifted to avoid overlaps. Left: $p_1(x) \sim \mathbf{1}\{x \in [0,1]^3\}$, $p_2(x) \sim \mathcal{N}(0, (1/3)^2\mathbf{I})$; Middle: $p_1(x) \sim \mathcal{N}(0, (1/2)^2\mathbf{I})$, $p_1(x) \sim \mathcal{N}(1, (1/2)^2\mathbf{I})$; Right: Beta mixture in (8).

We report their performance in Figure 6. For each of the three estimation problems described here, we experiment with 3 dimensional distributions and increasing sample sizes (the sample size, ranges from 50 to or more in logarithmic scale). Error bars are obtained by replicating each set-up 10 times. We see that co-BPM generally exhibits the best performance among the estimators considered. The estimates of NWJ-M1 and NWJ-M2 is somewhat less good and have larger variance; moreover, the convex program of NWJ-M1 or NWJ-M2 is computationally difficult because of the logarithm or entropy term and its scale increases rapidly with the sample size (Grant et al., 2008). However, PC$-k$ is more stable than NWJ and k seems to strike a balance between bias and variance—the higher k corresponds to

lower variance but larger bias, e.g., its variance is smallest when $k = 10$ in Figure 6; on the right plot, PC$-k$ produces negative estimates with small sample size since it can not guarantee positivity.

4.4 Examples with Dimensions > 3

There are few experiments in dimensions higher than 3 in previous work, even though most of the methods claim that there are no technical difficulties when dimensionality increases. The reason is because that their performance degrades fast as dimensionality increases. We demonstrate two additional examples with $d = 5, 10$ and assess the convergence rate empirically, the densities in our example are

$$p_1(x) = \frac{24}{25}\prod_{i=1}^{d}\beta_{1,5}(x_i) + \frac{1}{25}\mathbf{1}\{x \in [0,1]^d\}, p_2(x) = \frac{49}{50}\prod_{i=1}^{d}\beta_{5,1}(x_i) + \frac{1}{50}\mathbf{1}\{x \in [0,1]^d\}$$

The results are shown in Figure 7, the sample size is plotted on the log scale and the error bars are standard deviation of 10 replicas. For KL divergence, the estimates of (Nguyen et al., 2010) and (Pérez-Cruz, 2008) are also plotted for reference. There are several observations: (1) On the log scale, the estimates converge to true values almost linearly, and is comparable to the results of NWJ-M1; (2) NWJ-M1 is slightly better than NWJ-M2, which tends to underestimate the KL divergence. (3) PC$-k$ becomes inferior rapidly when the dimensionality goes up, especially in small sample size with large negative estimates. This is partially related to the sparseness in multi-dimensions which renders $k-$nearest neighbor density estimator ineffective (Givens and Hoeting, 2012). There is another noticeable phenomenon worth further investigation—the estimates goes down first then up as sample size increases. (4) Compared with previous examples, the estimates in dimensions ≤ 3 converge relatively faster than those when dimensions are 5 or 10, this degradation of convergence corroborates the already cited work, which corresponds to the difficulty in multivariate density estimation.

5 Conclusion and Discussion

A unified approach to estimating discrepancies of distributions is proposed from a Bayesian perspective. The joint prior provides a single-shot way to estimate the values and conduct statistical inferences; the simulations demonstrate its attractive empirical performance. In applications, this approach can be naturally extended to handle multiple-sample case, for example, given 3 samples $\mathcal{X}, \mathcal{Y}, \mathcal{Z}$ drawn from p_1, p_2, p_3 respectively and some distance measure $D(\cdot, \cdot, \cdot)$, we can estimate $D(p_1, p_2, p_3)$ according to $\mathcal{X}, \mathcal{Y}, \mathcal{Z}$ by binary-partitioning their sample space jointly when similar lower bound in Theorem 1 exists. The core of our methodology

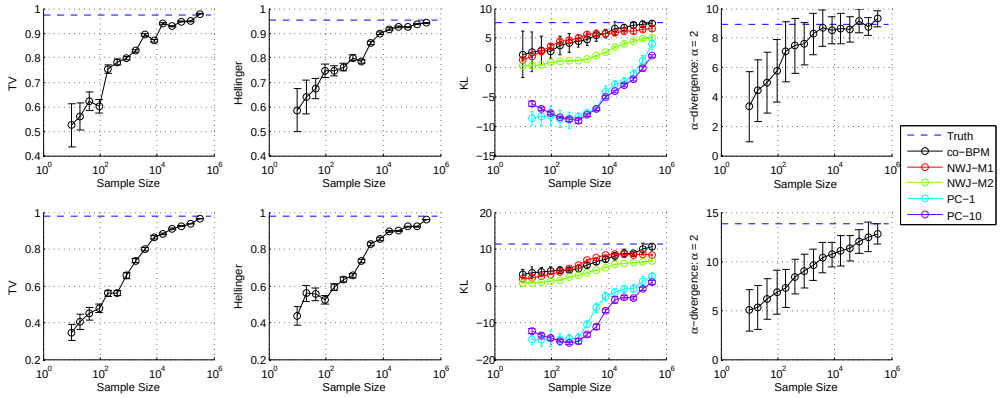

Figure 7: **Examples and comparison when dimensions > 3.** log(Sample size) vs. Divergences. Top: 5-dim example, the true values of Total Variation, Hellinger Distance, KL divergence and $\alpha-$divergence with $\alpha = 2$ are 0.9756, 0.9520, 7.6365, 8.9440 respectively. Bottom: 10-dim example, the true values are 0.9790, 0.9779, 11.3819, 13.8341.

is Theorem 1, which opens up the possibility to apply any domain partition based density estimators, a possible future direction is to use even more adaptive partitioning schemes.

References

Ali, S. and Silvey, S. D. (1966). A general class of coefficients of divergence of one distribution from another. *Journal of the Royal Statistical Society. Series B (Methodological)*, pages 131–142.

Chaloner, K. and Verdinelli, I. (1995). Bayesian experimental design: A review. *Statistical Science*, 10(3):273–304.

Donoho, D. L. and Grimes, C. (2003). Hessian eigenmaps: Locally linear embedding techniques for high-dimensional data. *Proceedings of the National Academy of Sciences*, 100(10):5591–5596.

Givens, G. H. and Hoeting, J. A. (2012). *Computational statistics*, volume 708. John Wiley & Sons.

Grant, M., Boyd, S., and Ye, Y. (2008). Cvx: Matlab software for disciplined convex programming.

Hastings, W. K. (1970). Monte carlo sampling methods using markov chains and their applications. *Biometrika*, 57(1):97–109.

Ho, P. J. M. P. P. and Vasconcelos, N. (2004). A kullback-leibler divergence based kernel for svm classification in multimedia applications. *Proc Adv Neural Inf Process Syst*, 16:1385–1392.

Leonenko, N., Pronzato, L., and Savani, V. (2008). A class of rényi information estimators for multidimensional densities. *The Annals of Statistics*, 36(5):2153–2182.

Ma, L. and Wong, W. H. (2011). Coupling optional pólya trees and the two sample problem. *Journal of the American Statistical Association*, 106(496).

Nguyen, X., Wainwright, M. J., and Jordan, M. I. (2010). Estimating divergence functionals and the likelihood ratio by convex risk minimization. *Information Theory, IEEE Transactions on*, 56(11):5847–5861.

Pérez-Cruz, F. (2008). Kullback-leibler divergence estimation of continuous distributions. In *Information Theory, 2008. ISIT 2008. IEEE International Symposium on*, pages 1666–1670. IEEE.

Póczos, B. and Schneider, J. G. (2011). On the estimation of alpha-divergences. In *International Conference on Artificial Intelligence and Statistics*, pages 609–617.

Póczos, B., Xiong, L., and Schneider, J. (2012). Nonparametric divergence estimation with applications to machine learning on distributions. *arXiv preprint arXiv:1202.3758*.

Sainudiin, R., Teng, G., Harlow, J., and Lee, D. (2013). Posterior expectation of regularly paved random histograms. *ACM Transactions on Modeling and Computer Simulation (TOMACS)*, 23(1):6.

Sricharan, K., Raich, R., and Hero III, A. O. (2010). Empirical estimation of entropy functionals with confidence. *arXiv preprint arXiv:1012.4188*.

Sugiyama, M., Kanamori, T., Suzuki, T., du Plessis, M. C., Liu, S., and Takeuchi, I. (2012). Density-difference estimation. In *NIPS*, volume 25, pages 692–700.

Wang, Q., Kulkarni, S. R., and Verdú, S. (2005). Divergence estimation of continuous distributions based on data-dependent partitions. *Information Theory, IEEE Transactions on*, 51(9):3064–3074.

Wang, Q., Kulkarni, S. R., and Verdú, S. (2009). Divergence estimation for multidimensional densities via-nearest-neighbor distances. *Information Theory, IEEE Transactions on*, 55(5):2392–2405.

Wong, W. H. and Ma, L. (2010). Optional pólya tree and bayesian inference. *The Annals of Statistics*, 38(3):1433–1459.